# Improvement of cooling performance and mitigation of fire propagation in lithium-ion batteries using a novel gas-cooled thermal management system

Pitsanusan Boonkit[1], Nontawee Petchsart[1], Supawut Apirakkitthworn[1] and Piyatida Trinuruk[1,*]

[1]*Department of Mechanical Engineering, King Mongkut's University of Technology Thonburi, Thailand*

**Corresponding author. Tel.: +66-2470-9114, Fax: +66-2470-9111*

*E-mail address: piyatida.tri@mail.kmutt.ac.th*

## Abstract

Development of battery thermal management systems has become significant because an inappropriate operating temperature is the primary cause of battery deterioration, fires and explosions. The current work proposes a revolutionary battery thermal management system that uses an inert gas instead of air as a coolant to increase cooling performance and avoid battery thermal runaway and fire propagation. The thermal behavior of 18650 cylindrical lithium-ion battery modules was assessed using a test station. The cooling performance of this battery thermal management system was investigated using Ansys Fluent, while the fire dynamics simulator assessed fire propagation when the battery was surrounded by various inert gas coolants. Inert gases can be more effective coolants than air. They were successful in lowering the maximum temperature and enhancing the convective heat transfer coefficient. Increased turbulent flow contributed in enhancement of heat transfer, as assessed by the Nusselt number. Although all gas coolants in this investigation effectively kept the cell temperature below 60 $^{o}$C, which is the starting temperature of thermal runaway, a high Reynolds number was necessary. Otherwise, helium is the best coolant for transferring heat from a battery even at extremely low Reynolds numbers. When the battery was surrounded by inert gas, fire propagation in the battery can be minimized. Use of an air-cooling system can initiate fires and explosions when battery thermal runaway occurs.

***Keywords:*** *Inert gas, Reynolds number, Nusselt number, Fire propagation, Thermal runaway*

## Nomenclature

| | | |
|---|---|---|
| $c_p$ | Specific heat (J kg$^{-1}$ °C$^{-1}$) |
| $h$ | Heat transfer coefficient (W m$^{-2}$ °C$^{-1}$) |
| $k$ | Thermal conductivity (W m$^{-1}$ °C$^{-1}$) |
| $L$ | Length of battery cell (m) |
| $Nu$ | Average Nusselt number (-) |
| $Pr$ | Prandtl number (-) |
| $q'''$ | Volumetric heat generation (W m$^{-3}$) |
| $Re$ | Reynolds number (-) |
| $T$ | Dimensionless temperature (-) |

| | | |
|---|---|---|
| $T^*$ | Temperature (°C) |
| $u$ | Velocity along the axial direction (m $s^{-1}$) |
| $U$ | Dimensionless velocity along the axial direction (-) |
| $v$ | Velocity along the transverse direction (m $s^{-1}$) |
| $V$ | Dimensionless velocity along the transverse direction (-) |
| $w$ | Half-width (m) |
| $W_s$ | Dimensionless width (-) |
| $x$ | Axial direction (m) |
| $X$ | Dimensionless axial direction (-) |
| $y$ | Transverse direction (m) |
| $Y$ | Dimensionless transverse direction (-) |

**Greek symbols**

| | |
|---|---|
| $\alpha$ | Thermal diffusivity of fluid ($m^2$ $s^{-1}$) |
| $v$ | Kinematic viscosity of the fluid ($m^2$ $s^{-1}$) |
| $\rho$ | Density of fluid (kg $m^{-3}$) |
| $\mu$ | Dynamic viscosity (N s $m^{-2}$) |

**Subscripts**

| | |
|---|---|
| *avg* | Average |
| *f* | Fluid domain |
| *m* | Mean |
| *max* | Maximum |
| *s* | Solid domain |
| ∞ | Free stream |

## 1. Introduction

Lithium-ion batteries (LIBs) are frequently used for electrochemical energy storage due to their high energy density, high discharge current, minimal self-discharge, and long-life cycle. Electric vehicles (EVs) are appealing applications that require significant discharge energy and current. These requirements are met owing to the excellent properties of LIBs. However, the biggest obstacle to widespread adoption of EVs is the distance range per charge (Alkhalidi et al., 2021). When batteries are improperly utilized, several thermal and safety risks can result in unforeseen problems, including thermal runaway, fire propagation, and battery explosion. When numerous battery cells are packed together to provide the required capacity, the magnitude of devastation caused by fire propagation and battery explosions is magnified and more likely to occur.

Several Battery Thermal Management System (BTMS) approaches have been documented in

past research. Lu et al. (2020) reviewed the traditional BTMS that employs an air-cooling system, which is a basic design that is feasible, safe, and dependable for any battery type. However, the BTMS does not benefit from air's low specific heat, low density, and poor thermal conductivity. Malik et al. (2018) demonstrated the thermal and electrical characteristics of a battery pack. According to this investigation, the optimum operating temperature range of the battery pack was 25 ºC–40 ºC, and the appropriate coolant temperature was 30 ºC. Such an air-cooling system was unable to sufficiently perform for a BTMS, so a direct BTMS employing refrigerant coolant was proposed. Park and Jung (2013) developed and analyzed air-type and liquid-type BTMS models. To maximize the use of space, the BTMS must service close spacing between cells on large battery packs. An air-type BTMS consumes less energy than a liquid-cooled system. By improving the design of structure and cell spacing in battery packs, multiple thermal management solutions have been established (Chen et al., 2018; Chen et al., 2019a). Ji et al. (2019) designed an appropriate battery cell configuration that changed cell spacing. The maximum battery temperature decreased with increased spacing. Several researchers optimized parameter configurations (Akinlabi and Solyali, 2020; Zhang et al., 2021a; Zhang et al., 2021b; Chen et al., 2017; Xie et al., 2017). Wang et al. (2021) employed a parallel plate to boost cooling efficiency, whereas Chen et al. (2019b) improved the thermal performance of various BTMS designs by developing the flow configuration and pattern of the cooling system.

The theory of energy transfer analysis was implemented to enhance BTMS performance. Realistic fluid flow analysis and conjugate heat transfer of an LIB prismatic cell was shown to be an excellent method for optimizing a BTMS to maintain a proper thermal condition. Afzal et al. (2021) developed a suitable BTMS by considering volumetric heat generation, the aspect ratio, conduction–convection parameters, Reynolds number, and cell spacing. Mokashi et al. (2020) investigated the maximum temperature of an LIB pack when different working fluids were used as coolants. The effects of the Reynolds number on cooling performance were analyzed.

Significant heat transfer is required to improve a thermal management system. Ideal coolant properties such as high thermal capacity, high conductivity, low viscosity, and non-toxicity are desirable to optimize a heat transfer process. Therefore, several inert gases, including helium (He) and carbon dioxide ($CO_2$), were proposed to improve cooling performance. Helium is an ideal inert coolant because it is a chemically inert gas with a high specific heat and thermal conductivity. Helium may play a key role as a coolant in some challenging applications, such as superconducting magnets and nuclear applications in both fusion and fission reactors (Baxi and Wong, 2000; Ranjithkumar et al., 2020; Donne et al., 1998). Even though an inert gas can reduce the intensity of fires and explosions with increased flame suppression, knowledge of inert gas-based cooling employed in electric vehicles is scant. Alipour et al. (2021) investigated and compared a cooling system for LIBs using helium-based cooling to one using air as a working fluid. Owing the ideal properties of helium, *i.e.*, better thermal conductivity and specific heat, helium coolant outperformed air-cooling. Mier et al. (2022) evaluated pressure build-up within a battery cell subjected to thermal abuse. A battery cell was placed in an enclosure that was charged with helium during testing to improve heat transmission. Wang et al. (2022) examined the behavior of gas released during thermal runaway. A battery cell was constructed within a pressure vessel filled with helium that was less than 1% air.

The challenge in LIBs is not only enhancement of energy density, but also addressing thermal issues which can negatively impact battery performance and induce battery thermal runaway. Thermal runaway often happens when the heat generated in the battery causes its temperature to exceed 60 ºC (Wang et al., 2019). As a result, experiments and numerical studies to analyze thermal runaway behavior of LIBs have been done to increase safety and minimize the negative effects of high temperature. Said and Tohir (2021) studied thermal runaway behavior and observed that higher battery capacity increased the likelihood of thermal runaway as well as providing for a shorter induction time. Chombo and Laoonual (2022) developed empirical equations to predict the onset of thermal runaway and analyze associated thermal hazard under external

heating-to-failure circumstances. The state of charge (SOC) and battery chemistry were two parameters investigated to validated the model's accuracy. Zhang et al. (2022) focused on the composition of gas produced during thermal runaway. It was discovered that when the battery's SOC was increased, more types of exhaust gases were generated, directly affecting thermal hazards. Weng et al. (2021) used battery packs to evaluate the influence of oxygen concentration and dilution gases on thermal runaway behavior. Lowering the oxygen level by dilution with an inert gas (argon or nitrogen), can delay thermal runaway. The strategy of oxygen limitation in a battery to minimize thermal runaway was also examined by Barelli et al. (2021).

Another unanticipated risk posed by LIBs is the propagation of fire and heat. Thermal runaway from a triggered cell to adjacent cells promotes fire propagation, and massive amounts of heat can be released. Eshetu et al. (2013) analyzed the combustible components of LIBs. The liquid electrolyte accounted for a significant portion of the overall energy produced from combustion during thermal runaway (at least 50%). Srinivasan et al. (2020) discovered that dimethyl carbonate (DMC) had the lowest boiling point, 90 ºC, producing a significant impact on fire propagation. The total energy released by a battery explosion was computed by Zhao et al. (2020). Chen et al. (2015) evaluated the fire characteristics of two 18650 LIBs, lithium cobalt oxide (LCO) and lithium iron phosphate (LFP). They found that LIB fire hazards were often caused by continual heating and internal heat generation *via* exothermic processes. Fu et al. (2015) investigated the burning characteristics of LIBs. The peak heat release rate and hazardous gas concentrations rose dramatically as SOC increased, whereas the period to ignition and time to explosion were reduced. The use of gases such as $CO_2$ and $N_2$ to control fire propagation in LFP batteries was investigated by Weiqiang et al. (2018). Their study found that $CO_2$ can control fires to a greater degree than nitrogen ($N_2$) because it is an inert gas with a higher heat absorption capacity. However, inert gas cannot completely extinguish a fire since a battery cell can be re-ignited after the flames are quenched. Thermal abuse and thermal runaway behavior of LIBs within a battery pack were investigated by Li et al. (2022). In terms of thermal runaway and its propagation, there was some variation in the battery modules within the enclosure. Mukhopadhyay et al. (2023) investigated air-precooling with a water mist for thermal runaway management. Mist precooling tended to limit thermal runaway.

Research on the use of inert gas as a coolant for battery thermal management purposes has increasingly been done due to their unique properties. However, most studies concentrated on the effects of a few types of inert gases on cooling performance. Therefore, the novelty of the current study lies in its proposed use of inert gas as an alternative coolant for a BTMS. This is a novel approach to the traditional air-cooled system has the potential to increase heat transfer while mitigating the risk of battery explosions. Helium (He), carbon dioxide ($CO_2$), nitrogen ($N_2$), and argon (Ar) were used as coolants instead of air owing to their superior thermal properties. Furthermore, the use of inert gases was meant to alleviate safety concerns because they are neither combustible not poisonous. They are ecologically benign and do not support chemical reactions that promote fire propagation. The capabilities of an inert gas-based cooled BTMS to suppress fires and increase cooling performance were investigated in this study. An air-cooling experiment on a battery module was performed to evaluate model accuracy. Ansys Fluent was employed as a simulation tool to assess the cooling performance of a BTMS. The effect of the Reynolds number was investigated and a parametric study was done for various inert gases. Dimensionless local and average Nusselt numbers were used to elucidate the heat transfer characteristics. A fire dynamics simulator was employed to examine battery explosions in a fire suppression investigation.

## 2. Methodology

Experiments and a numerical simulation were carried out in the current study to investigate

the thermal performance of a BTMS and to assess its fire suppression capabilities when various inert gases were used instead of a conventional air coolant. The experiment was design to collect data for validating model accuracy in a battery air-cooling system, whereas numerical simulation was used to examine the fire suppression capabilities during battery combustion and cooling performance when an inert gas was used as coolant.

### *2.1. Experimental configuration of an air-cooled battery thermal management system*

BTMS cooling performance was experimentally investigated using air as a coolant, whereas use of inert gas coolants, such as He, $CO_2$, $N_2$ and Ar, for thermal management and fire suppression was explored numerically. The thermophysical properties of five coolant gases in this study are summarized in Table 1. Helium has an advantage in terms of heat transfer characteristics due to its higher specific heat and thermal conductivity. An experiment was done to validate model accuracy. Figure 1 shows the experimental configuration of the battery air-cooling system used in the current study. TORIYAMA LIBs NMC 18650 cylindrical cells were employed in this investigation. A cell's nominal capacity, nominal voltage, and cut-off voltage were 2500 mAh, 3.6 V, and 4.2 V, respectively. The battery modules were connected 5 in series and 4 in parallel. The test section consisted of a centrifugal blower, electronic load, and data acquisition system. A straightener was installed to ensure consistency of the airflow velocity profile and homogeneity of heat dissipation conditions of battery cells, since a uniform airflow distribution was necessary. T-type thermocouples were attached at the center of each cell to monitor cell surface temperatures. The experiment was done at a discharge rate of 1C using ambient air as a coolant to validate the experimental results compared to the simulation.

### *2.2. Simulation model of battery thermal management system*

The thermal performance of a BTMS using an inert gas and air cooling was investigated with Computational Fluid Dynamics (CFD) Ansys Fluent. Heat generation in each battery cell was determined by conducting a single cell discharge experiment at the discharge rate of 1C. A parametric study on the effect of the Reynolds numbers in the 500 – 30000 range on the thermal performance of battery modules was conducted. The average temperature and pressure drop across the battery module were calculated, and the local Nusselt number was evaluated to compare the heat transfer performance of different coolants at various flow velocities.

Figure 2(a) shows a physical model of a BTMS with 20-cylindrical cells packed and configured in an aligned arrangement. The coolant flowed parallel and uniformly through the module. Heat generation in each cell was considered uniform (Karimi and Li, 2013). Thermal-hydraulic analysis of conjugated heat transfer in the cooling channel used dimensionless temperatures ($T$) and local Nusselt numbers ($Nu_x$).

### *2.3 Physical model of fire propagation*

A fire dynamics simulator was employed to observe the mitigation of fire propagation within a battery when it was surrounded by a gas coolant. A model of a single LIB cell in an enclosure was created. The dimensions of enclosure were 1.2 × 1.2 × 1.2 m (Chen et al. 2015; Lin et al. 2017) and the interior was filled with a gas coolant, as shown in Figure 2(b). The heat input profile acquired from the thermal runaway of a 18650 lithium-ion battery at a 100% SOC (Chen et al., 2015) was used to force the battery into combustion in the fire dynamics simulator. A thermocouple was mounted 3 cm above the battery to examine the flame temperature. The capability of fire suppression by various inert gases was investigated through the heat release rate (HRR) and temperature distribution. An adiabatic boundary condition was devised to confine the system.

## 3. Governing equations

Whether the battery was cooled by natural or forced convection, the core temperature of a cylindrical cell is higher than its surface temperature (Veneri, 2017). The core temperature should be kept under the safe limit since it will produce a hazard condition. A BTMS is, thus, a safety consideration. To investigate the performance of a BTMS, the governing equation characterizing the heat transfer process is given as,

$$k_s \nabla^2 T + q''' = \rho c_p \nabla^2 T + h \nabla^2 T \tag{1}$$

Fluid density was assumed to remain constant in this investigation. It was neither compressed nor expanded in the simulation. An incompressible fluid flow model with forced convection was applied. The continuity equation serves as the governing equation in the fluid domain. The mass, momentum, and energy conservations statements are,

$$\nabla u = 0 \tag{2}$$

$$(u \nabla u) = -\frac{1}{\rho} \nabla p + \mu \nabla^2 u \tag{3}$$

$$u \nabla T = \alpha \nabla^2 T \tag{4}$$

Dimensionless temperature ($T$) is given as,

$$T = \frac{T^* - T_\infty}{T_0 - T_\infty} \tag{5}$$

where $T_0$ is allowable maximum temperature and $T_\infty$ is free stream temperature.

Dimensionless axial and transverse directions can be calculated as,

$$X = \frac{x}{L} \tag{6}$$

$$Y = \frac{y}{w} \tag{7}$$

Newton's law of cooling at the cell/coolant interface is,

$$-k \frac{\partial T}{\partial Y}\Big|_{y_s = w_s} = h\left(T^*_{y_s = w_s} - T^*_{f,m}\right) \tag{8}$$

A dimensionless Nusselt number is used in this study to characterize the convective heat transfer coefficient at a battery surface within a coolant fluid. The local Nusselt number ($Nu_x$) at the cell surface is obtained, while integration of $Nu_x$ throughout the cell surface length provides the average Nusselt number ($Nu_{avg}$), as presented in Equations (9) and (10).

$$Nu_x = -\frac{1}{(T_{Y_S = W_S} - T_{f,m})} \frac{\partial T}{\partial Y}\Big|_{Y_S = W_S} \tag{9}$$

$$Nu_{avg} = -\int_0^1 \frac{1}{(T_{Y_S = W_S} - T_{f,m})} \frac{\partial T}{\partial Y}\Big|_{Y_S = W_S} dX \tag{10}$$

where $T_{f,m}$ is the dimensionless mean temperature of the fluid domain and $T_{Y_S = W_S}$ is the dimensionless cell surface temperature.

The average Nusselt number may be expressed as a function of the Reynolds ($Re$) and Prandtl ($Pr$) numbers. Nusselt and Reynolds numbers can be related through the convective heat transfer coefficient ($h$), which is impacted by flow conditions. The Prandtl number, which is the ratio of the

momentum diffusivity to thermal diffusivity, influences the convective heat transfer coefficient. Therefore, the Nusselt number correlation can express the relationship between the Reynolds and Prandtl numbers as,

$$Nu_{avg} = c\, Re^m Pr^n \tag{11}$$

where $c, m$ and $n$ are constants that can be varied depending on the system geometry and flow conditions.

## 4. Result and discussion

### *4.1 Simulation validation and verification testing*

#### *4.1.1 Model validation of an air-cooled battery thermal management system*

For model validation, the BTMS test section using air as a coolant was tested at a 1C discharge rate with an air velocity of 4 m/s (Re = 19250). As shown in Figure 3(a), the experimental results of average battery module temperature were in good agreement with the numerical results. The mean error was less than 3%, which is considered acceptable.

#### *4.1.2 Model validation of fire dynamics simulation*

To evaluate the correctness of fire dynamics simulation model, the heat input acquired from Chen et al. (2015) was utilized as a heat source to compute the fire dynamics simulator's heat release rate (HRR). Figure 3(b) shows the HRR profile of the simulation results and observations in the literature, which are in good agreement. There were two HRR peaks visible that correlated well with Chen et al. (2015). The magnitude of the first energy release was 1.5 kW, while the second energy release was roughly 8 kW.

### *4.2 Characteristics of temperature and local Nusselt number*

The dimensionless temperature and local Nusselt number were comparatively examined to assess the heat transfer characteristics of different gas coolants. When fluid is flowed across a single circular cylinder, flow separation and vortex shedding can occur. The separation of a boundary layer can affect the heat transfer characteristics, as demonstrated by the undershoot of the Nusselt number between $80° \leq \theta \leq 100°$ (Park et al., 2015). In this investigation, $\theta = 90°$ was chosen to explore the trend of heat transfer. The fluid temperature distribution was illustrated in dimensionless terms by calculating the permitted maximum temperature at 60 ºC as a safe limit. Battery operation over this temperature limit may result in thermal runaway.

Figures 4(a) and 4(b) illustrate the local temperature distribution along a flow channel when air or helium is employed as a coolant. Although the dimensionless temperature trend was consistent across all coolants, the magnitude varied. The maximum temperature occurred at the battery surface ($Y_f = 0$) and the temperature decreased in the transverse direction along the flow channel. By increasing the Reynolds number to enhance turbulent flow, greater heat transfer and a lower temperature gradient resulted. The temperature distribution was considerably decreased when the flow was in laminar and transition regimes with Reynolds numbers between 500 and 5000. Increased fluid velocity in the turbulent regime with Reynolds numbers more than 5000, on the contrary, could not clearly produce a difference in the temperature gradient between the solid surface and the fluid.

Figures 4(c) and 4(d) show the distribution of the local Nusselt number over the width of the flow channel for air and helium coolants as a function the Reynolds number. An increased Reynolds number resulted in more convective heat transfer and a higher Nusselt number. The Reynolds number was impacted by temperature, indicating improved heat transfer. At Reynolds numbers higher than

5000, the maximum Nusselt number occurred on the battery surface. When the coolant was in laminar flow or the Reynolds numbers was less than 5000, the maximum Nusselt number emerged in the fluid near the surface. At a low Reynolds number, the influence of the boundary layer, which had viscous force within the fluid, was slightly more than the inertial force. As the Reynolds number increased, the inertial force easily overcame the viscous force.

### *4.3 Effect of Reynolds numbers on the heat transfer characteristics*

The effect of Reynolds numbers on the maximum dimensionless temperature ($T_{max}$) at the battery surface with varied coolants is illustrated in Figure 5. The results clearly demonstrated that increasing the Reynolds number decreased the maximum battery temperature. High flow velocity introduced a high convective heat transfer coefficient, which reduced the boundary layer effect. In these cases, the viscous force dominated the inertial force. The heat transfer performance was poorest when argon was used as a gas coolant. All gas coolants, with the exception of helium, can keep the maximum temperature within the safe limit at $T_{max}$ = 1, but they must exceed a certain Reynolds number. To protect the battery from thermal runaway, each gas coolant required its own minimal critical Reynolds number, which was used to assess whether the battery temperature was below the safe limit. The minimum critical Reynolds number for air was 1880, whereas other coolants had values of 1829 for $N_2$, 2086 for $CO_2$, and 3121 for Ar. However, helium has excellent thermal performance for thermal management as it can keep the maximum temperature below the safe limit at all Reynolds numbers. This was because helium has a high specific heat and thermal conductivity, which distinguished it from the other coolants, as shown in Table 1. Then, a gas coolant with superior characteristics, such as helium, may better transfer heat away from the battery.

Figure 6 illustrates how the Reynolds number affects the average Nusselt number at the battery surface in various gas coolants. An increased Reynolds number resulted in an enhanced average Nusselt number due to a greater convective heat transfer coefficient. However, there was no discernible variation in the average Nusselt number when various gas coolants were applied, including helium, which is definitely indicated by lowest maximum temperatures in Figure 5. This was because the average Nusselt number, given in Equation (10), is a function of the temperature gradient in the boundary layer ($T_{Y_s=W_s} - T_{f,m}$) and the temperature derivative at the solid-fluid interface ($\left(\frac{\partial T}{\partial Y}\right|_{Y_s=W_s}$). Helium had a smaller temperature gradient and a larger temperature derivative for the same Reynolds number and axial direction than other gases. The average Nusselt number of all coolants was not significantly different, despite helium's superior heat transfer capability. Helium can hold more heat with a smaller temperature increase due to its high specific heat. An empirical formula for the Nusselt number and inert gas-cooled BTMS, Equation (12), was developed using simulation results utilizing four types of inert gases and air. The multiple R-squared value was used to validate the significance of correlation between $Nu_{avg}$, $Re$ and $Pr$. The multiple R-squared from the numerical data of all gas coolants in this study was 0.9878, indicating a strong correlation between three variables.

$$Nu_{avg} = 0.031\, Re^{0.595} Pr^{0.2} \tag{12}$$

### *4.4 Pressure drop in the system*

Assessment of the thermal performance of inert gas-based BTMSs was evaluated not only on the basis of temperature and heat transfer characteristics, but also as a function of pressure drop throughout the system. This has a direct influence on the energy consumption of the turbomachinery conveying the coolant fluid. Figure 7 displays the pressure drop of the system with different gas coolants flowing through the battery module. Due to relatively low density of helium gas, its use exhibits a substantial pressure drop compared to other gases. As a result, helium must operate at a

very high flow velocity to achieve the same Reynolds number, which promotes a high pressure drop in the system. As a consequence, helium may become an unattractive coolant on the basis the Reynolds number alone. However, when the safe limit temperature was considered, helium was only coolant that could function at very low Reynolds numbers, starting at Re=500. Other coolants had a minimum Reynolds number of roughly 2000. Therefore, helium was an effective and high-quality coolant for managing heat transfer in a battery module. while also having minimal influence on pressure drop.

### *4.5 Fire propagation*

The simulation results of the flame temperature measured above the cell, as well as the temperature contours at various time steps, are provided to analyze the capability of the inert gas coolant in fire suppression. Figure 8 shows the flame temperature after a battery cell was forced into thermal runaway by applying heat. The results clearly show that an air coolant promotes battery combustion. As a result, fire spread. However, inert gases could restrain combustion. Nonetheless, an increased temperature was observed in these cases due to the radiation impact of heat input. In the case of air, the peak temperatures at the first and second energy releases were 600 ºC and 750 ºC, respectively, which correspond with the heat input and the temperature distribution, as seen in Figure 9. A suppression of temperature in the case of a helium coolant was observed since helium has a lower density and a greater specific heat.

## 5. Conclusions

This study proposed a novel alternative BTMS using an inert gas as a coolant, such as helium, carbon dioxide, nitrogen, or argon, instead of air to minimize degradation of the battery lifespan and prevent battery combustion due to operation at an unsafe temperature. The following are the current study's findings:

- Using inert gas as a coolant instead of air can significantly improve the thermal performance of a BTMS. Helium is the best coolant since it could suppress the battery module's temperature, preventing thermal runaway at all Reynolds numbers. Conversely, argon, is the poorest coolant.
- The minimum critical Reynolds number for air was 1880. It was 1829 for nitrogen, 2086 for carbon dioxide, and 3121 for argon. These Reynolds numbers were the minimum necessary to keep the battery temperature below the allowable safe limit.
- Using helium can result in a higher pressure drop. However, helium can function at a very low Reynolds number, 500, to keep the battery from thermal runaway. Other coolants must function at higher Reynolds numbers with greater pressure drops.
- Filling the enclosure with inert gas can help to prevent fire propagation, even if the flame temperature increases without battery explosion.

Finally, an inert gas can significantly increase thermal performance while also lowering the risk of thermal runaway and fire propagation. However, further development of this type of BTMS in conjunction with an inert gas-based cooling system is required before it can be employed in electric vehicles.

## 6. Recommendations

Helium has been found the best coolant for temperature reduction, thermal runaway prevention and fire propagation mitigation in lithium-ion batteries. However, there are technical and economic considerations that must be properly considered before helium-cooled BTMSs are

commercially deployed in EVs. In terms of economic feasibility, helium is in rather limited supply and it is expensive. Additionally, a specialized infrastructure for handling and transferring helium is necessary, which may increase the overall cost of implementing this technology. Nonetheless, the long-term benefits of helium-cooled BTMS can offset these expenditures. Technically, a helium-cooled system must be a closed system to control pressure and prevent leakage from the battery pack and its system. This technology may encounter regulatory challenges since the use of a pressurized system in EVs is subject to safety regulations that vary by country. Additionally, helium is a controlled material under some national regulations. Nevertheless, the long-term benefits of using inert gases, such as increased battery life and improved safety, may outweigh the initial cost of deploying such cooling technology.

**Acknowledgements**

The authors acknowledge the supported provided by National Science and Technology Development Agency (NSTDA) under the Research Chair Grant, and Thailand Science Research and Innovation (TSRI) Basic Research Fund: Fiscal year 2023 under Project Number FRB660073/0164 (Program Sustainable Mobility).

**References**

Afzal, A., Abidi, A., Ad, M., Rk, A., Soudagar, M. and Saleel, A., Effect of Parameters on Thermal and Fluid-Flow Behavior of Battery Thermal Management System, *Therm. Sci.*, vol. **25**, no. 5 Part B, pp. 3775–87, 2021. DOI: 10.2298/TSCI191206290A

Akinlabi, A.A.H. and Solyali, D., Configuration, Design, and Optimization of Air-Cooled Battery Thermal Management System for Electric Vehicles: A Review, *Renew. Sust. Energ. Rev.*, vol. **125**, 109815, 2020. DOI: 10.1016/j.rser.2020.109815

Alipour, M., Hassanpouryouzband, A. and Kizilel, R., Investigation of the Applicability of Helium-Based Cooling System for Li-Ion Batteries, *Electrochem.*, vol. **2**, no. 1, pp. 135–48, 2021. DOI: 10.3390/electrochem2010011

Alkhalidi, A., Almahmood, R., Malkawi, H. and Amano, R. S., What are the Barriers that Prevent Its Adoption? Case Study of Battery Electric Vehicles, *Inter. J. Energy Clean Environ.,* vol. **22**, no. 1, pp. 1–14, 2021. DOI: 10.1615/InterJEnerCleanEnv.2020035391

Barelli, L., Bidini, G., Gallorini, F., Ottaviano, P. A., Pelosi, D., Perla, M. and Serangeli, M., Oxygen Reduction Approaches for Fire Protection to Increase Grid Li-Ion BESS Safety, *E3S Web of Conferences*, vol. **238**, 09001, 2021. DOI: 10.1051/e3sconf/202123809001

Baxi, C.B. and Wong, C.P.C., Review of Helium Cooling for Fusion Reactor Applications, *Fusion Eng. Des.*, vol. **51–52**, pp. 319–24, 2000. DOI: 10.1016/S0920-3796(00)00336-7

Chen, K., Chen, Y., Li, Z., Yuan, F. and Wang, S., Design of the Cell Spacings of Battery Pack in Parallel Air-Cooled Battery Thermal Management System, *Int. J. Heat Mass Tran.*, vol. **127**, pp. 393–401, 2018. DOI: 10.1016/j.ijheatmasstransfer.2018.06.131

Chen, K., Song, M., Wei, W. and Wang, S., Design of the Structure of Battery Pack in Parallel Air-Cooled Battery Thermal Management System for Cooling Efficiency Improvement, *Int. J. Heat Mass Tran.*, vol.**132**, pp.309–21, 2019a. DOI:10.1016/j.ijheatmasstransfer.2018.12.024

Chen, K., Wang, S., Song, M. and Chen, L., Configuration Optimization of Battery Pack in Parallel Air-Cooled Battery Thermal Management System Using an Optimization Strategy, *Appl. Therm. Eng.*, vol. **123**, pp. 177–86, 2017. DOI: 10.1016/j.applthermaleng.2017.05.060

Chen, K., Wu, W., Yuan, F., Chen, L. and Wang, S., Cooling Efficiency Improvement of Air-Cooled Battery Thermal Management System through Designing the Flow Pattern, *Energy*, vol. **167**, pp. 781–90, 2019b. DOI: 10.1016/j.energy.2018.11.011

Chen, M., Zhou, D., Chen, X., Zhang, W., Liu, J., Yuen, R. and Wang, J., Investigation on the Thermal

Hazards of 18650 Lithium Ion Batteries by Fire Calorimeter, *J. Therm. Anal. Calorim.*, vol. **122**, no. 2, pp. 755–63, 2015. DOI: 10.1007/s10973-015-4751-5

Chombo, P.V. and Laoonual, Y., Prediction of the Onset of Thermal Runaway and Its Thermal Hazards in 18650 Lithium-Ion Battery Abused by External Heating, *Fire Safety J.*, vol. **129**, 103560, 2022. DOI: 10.1016/j.firesaf.2022.103560

Donne, M.D., Albrecht, H., Boccaccini, L.V., Fischer, U., Gordeev, S., Hutter, E., Kleefeldt, K., Norajitra, P., Reimann, G., Ruatto, P., Schlesiek, K. and Schnauder, H., European Helium Cooled Pebble Bed Blanket: Design of Blanket: Module to Be Tested in ITER, *Fusion Eng. Des.*, vol. **39–40**, pp. 825–33, 1998. DOI: 10.1016/S0920-3796(97)00158-0

Eshetu, G.G., Grugeon, S., Laruelle, S., Boyanov, S., Lecocq, A., Bertrand, J.P. and Marlair, G., In-Depth Safety-Focused Analysis of Solvents Used in Electrolytes for Large Scale Lithium Ion Batteries, *Phys. Chem. Chem. Phys.*, vol. **15**, no. 23, 9145, 2013. DOI: 10.1039/c3cp51315g

Fu, Y., Lu, S., Li, K., Liu, C., Cheng, X. and Zhang, H., An Experimental Study on Burning Behaviors of 18650 Lithium Ion Batteries Using a Cone Calorimeter, *J. Power Sources*, vol. **273**, pp. 216–22, 2015. DOI: 10.1016/j.jpowsour.2014.09.039

Ji, C., Wang, B., Wang, S., Pan, S., Wang, D., Qi, P. and Zhang, K., Optimization on Uniformity of Lithium-Ion Cylindrical Battery Module by Different Arrangement Strategy, *Appl. Therm. Eng.*, vol. **157**, 113683, 2019. DOI: 10.1016/j.applthermaleng.2019.04.093

Karimi, G. and Li, X., Thermal Management of Lithium-Ion Batteries for Electric Vehicles: Thermal Management of Li-Ion Battery Packs, *Inter. J. Energy Res.*, vol. **37**, no. 1, pp. 13–24, 2013. DOI: 10.1002/er.1956

Li, Z., Guo, Y. and Zhang, P., Effects of the Battery Enclosure on the Thermal Behaviors of Lithium-Ion Battery Module during Thermal Runaway Propagation by External-Heating, *J. Ener. Stor.*, vol. **48**, 104002, 2022. DOI: 10.1016/j.est.2022.104002

Lin, X., He, Y., Jiang, W., Liu, J., Chen, M., Yao, W., Ma, P., Ding, C. and Wang, J., Prediction of Heat Release Rate of Shredded Paper Tapes Based on Profile Burning Surface, *J. Therm. Anal. Calorim.*, vol. **130**, no. 3, pp. 2215–25, 2017. DOI: 10.1007/s10973-017-6517-8

Lu, M., Zhang, X., Ji, J., Xu, X. and Zhang, Y., Research Progress on Power Battery Cooling Technology for Electric Vehicles, *J. Ener. Stor.*, vol. **27**, 101155, 2020. DOI: 10.1016/j.est.2019.101155

Malik, M., Dincer, I., Rosen, M. A., Mathew, M. and Fowler, M., Thermal and Electrical Performance Evaluations of Series Connected Li-Ion Batteries in a Pack with Liquid Cooling, *Appl. Therm. Eng.*, vol. **129**, pp. 472–81, 2018. DOI: 10.1016/j.applthermaleng.2017.10.029

Mier, F.A., Hill, S.M. M., Lamb, J. and Hargather, M.J., Non-Invasive Internal Pressure Measurement of 18650 Format Lithium Ion Batteries during Thermal Runaway, *J. Energy Storage*, vol. **51**, pp. 104322, July 2022. DOI: 10.1016/j.est.2022.104322

Mokashi, I., Khan, S.A., Abdullah, N.A., Bin Azami, M.H. and Afzal, A., Maximum Temperature Analysis in a Li-Ion Battery Pack Cooled by Different Fluids, *J. Therm. Anal. Calorim.*, vol. **141**, no. 6, pp. 2555–71, 2020. DOI: 10.1007/s10973-020-10063-9

Mukhopadhyay, A., Jana, A., Saha, R., Pal, D. and Sarkar, S., Early Detection and Management of Thermal Runaway in Batteries Using Water Mist for Air Precooling, *Inter. J. Energy Clean Environ.*, vol. **24** (4), pp. 1-16, 2023. DOI: 10.1615/InterJEnerCleanEnv.2022043273

Park, J. M., Kim, O.J., Kim, S.J. and Shin, Y.C., Heat Transfer Characteristics of Circular and Elliptic Cylinders in Cross Flow, *Adv. Mech. Eng.*, vol. **7**, no. 11, 168781401561955, 2015. DOI: 10.1177/1687814015619553

Park, S. and Jung, D., Battery Cell Arrangement and Heat Transfer Fluid Effects on the Parasitic Power Consumption and the Cell Temperature Distribution in a Hybrid Electric Vehicle, *J. Power Sources*, vol. **227**, pp. 191–98, 2013. DOI: 10.1016/j.jpowsour.2012.11.039

Ranjithkumar, S., Yadav, B.K., Saraswat, A., Chaudhuri, P., Kumar, E.R., Kunze, A. and Ghidersa, B.E., Performance Assessment of the Helium Cooled First Wall Mock-up in HELOKA

Facility, *Fusion Eng. Des.*, vol. **150**, 111319, 2020. DOI: 10.1016/j.fusengdes.2019.111319
Said, M.S.M., and Tohir, M.Z.M., Characterisation of Thermal Runaway Behaviour of Cylindrical Lithium-Ion Battery using Accelerating Rate Calorimeter and Oven Heating, *Case Studies in Therm. Eng.*, vol. **28**, 101474, 2021. DOI: 10.1016/j.csite.2021.101474
Srinivasan, R., Thomas, M.E., Airola, M.B., Carkhuff, B.G., Frizzell-Makowski, L.J., Alkandry, H., Reuster, J.G., Oguz, H.N., Green, P.W., Favors, J.L., Currano, L.J. and Demirev, P.A., Preventing Cell-to-Cell Propagation of Thermal Runaway in Lithium-Ion Batteries, *J. Electrochem. Soc.*, vol. **167**, no. 2, 020559, 2020. DOI: 10.1149/1945-7111/ab6ff0
Veneri, O.E., *Technologies and Applications for Smart Charging of Electric and Plug-in Hybrid Vehicles*, Cham: Springer International Publishing, 2017.
Wang, H., Xu, H., Zhang, Z., Wang, Q., Jin, C., Wu, C., Xu, C., Hao, J., Sun, L., Du, Z., Li, Y., Sun, J., Feng, X., Fire and Explosion Characteristics of Vent Gas from Lithium-Ion Batteries after Thermal Runaway: A Comparative Study, *eTransportation*, vol. **13**, 100190, 2022. DOI: 10.1016/j.etran.2022.100190
Wang, J., Huang, W., Pei, A., Li, Y., Shi, F., Yu, X. and Cui, Y., Improving Cyclability of Li Metal Batteries at Elevated Temperatures and its Origin Revealed by Cryo-Electron Microscopy, *Nat. Energy*, vol. **4**, no. 8, pp. 664–70, 2019. DOI: 10.1038/s41560-019-0413-3
Wang, M., Teng, S., Xi, H. and Li, Y., Cooling Performance Optimization of Air-Cooled Battery Thermal Management System, *Appl. Therm. Eng.*, vol. **195**, 117242, 2021. DOI: 10.1016/j.applthermaleng.2021.117242
Weiqiang, Z., Shunbing, Z., Xun, L., and Xuetong, H., Experimental Study on Suppression of Fire and Explosion of Lithium Iron Phosphate Battery by Inert Gas, *2018 IEEE Int. Conf. Safety Produce Informatization (IICSPI)*, Chongqing, China: IEEE, pp. 57–61, 2018. DOI: 10.1109/IICSPI.2018.8690468
Weng, J., Ouyang, D., Liu, Y., Chen, M., Li, Y., Huang, X. and Wang, J., Alleviation on Battery Thermal Runaway Propagation: Effects of Oxygen Level and Dilution Gas, *J. Power Sources*, vol. **509**, 230340, 2021. DOI: 10.1016/j.jpowsour.2021.230340
Xie, J., Ge, Z., Zang, M. and Wang, S., Structural Optimization of Lithium-Ion Battery Pack with Forced Air Cooling System, *Appl. Therm. Eng.*, vol. **126**, pp. 583–93, 2017. DOI: 10.1016/j.applthermaleng.2017.07.143
Zhang, F., Yi, M., Wang, P. and Liu, C., Optimization Design for Improving Thermal Performance of T-Type Air-Cooled Lithium-Ion Battery Pack, *J. Energy Storage*, vol. **44**, 103464, 2021a. DOI: 10.1016/j.est.2021.103464
Zhang, Q., Liu, T. and Wang, Q., Experimental Study on the Influence of Different Heating Methods on Thermal Runaway of Lithium-Ion Battery, *J. Energy Storage*, vol. **42**, 103063, 2021b. DOI: 10.1016/j.est.2021.103063
Zhang, Q., Niu, J., Zhao, Z. and Wang, Q., Research on the Effect of Thermal Runaway Gas Components and Explosion Limits of Lithium-Ion Batteries under Different Charge States, *J. Energy Storage*, vol. **45**, 103759, 2022. DOI: 10.1016/j.est.2021.103759
Zhao, C., Sun, J. and Wang, Q., Thermal Runaway Hazards Investigation on 18650 Lithium-Ion Battery Using Extended Volume Accelerating Rate Calorimeter, *J. Energy Storage*, vol. **28**, 101232, 2020. DOI: 10.1016/j.est.2020.101232

**Table 1** Properties of various coolant gases at 27 ºC

| Coolant | Density ($kg\,m^{-3}$) | Specific heat ($kJ\,kg^{-1}\,°C^{-1}$) | Viscosity ($10^{-5}\,N\,s\,m^{-2}$) | Thermal conductivity ($W\,m^{-1}\,°C^{-1}$) | Pr (-) |
|---|---|---|---|---|---|
| Air | 1.167 | 1.005 | 1.855 | 0.025 | 0.7329 |
| Argon | 1.623 | 0.521 | 2.275 | 0.017 | 0.6636 |
| Carbon dioxide | 1.796 | 0.853 | 1.503 | 0.016 | 0.7635 |
| Helium | 0.162 | 5.193 | 1.994 | 0.156 | 0.7174 |
| Nitrogen | 1.138 | 1.041 | 1.790 | 0.026 | 0.6649 |

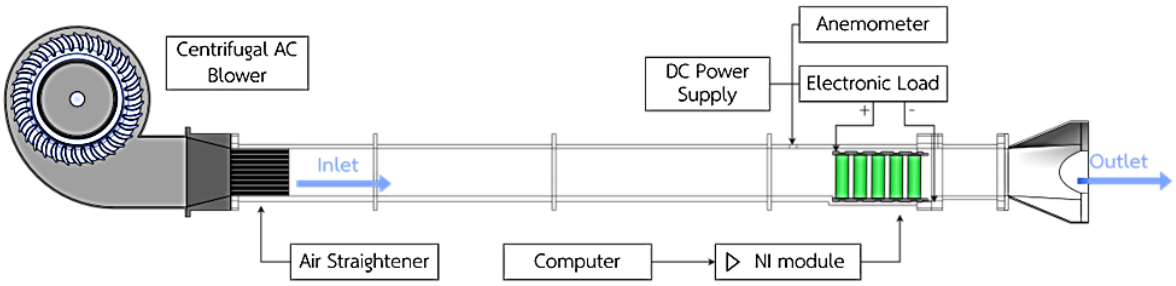


**Figure 1** Experimental configuration of an air-cooled battery thermal management system.

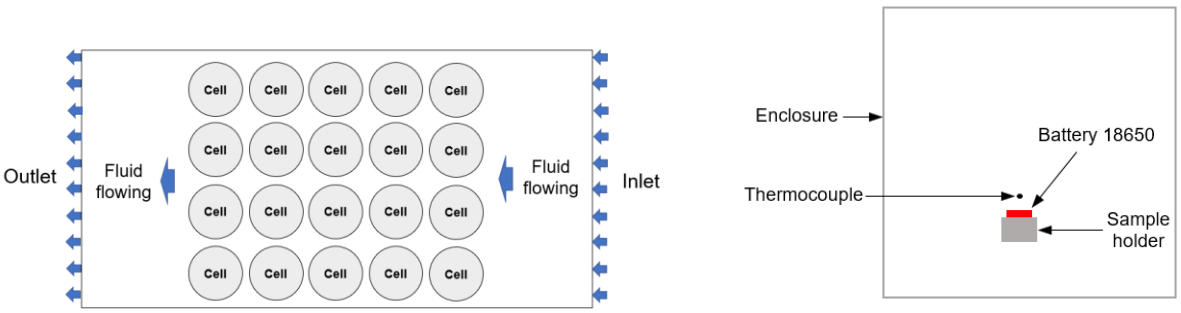


(a) Model of battery module for heat transfer analysis (b) Model of a battery cell in an enclosure

**Figure 2** Simulation models (a) battery module for heat transfer analysis and (b) a battery cell in an enclosure.

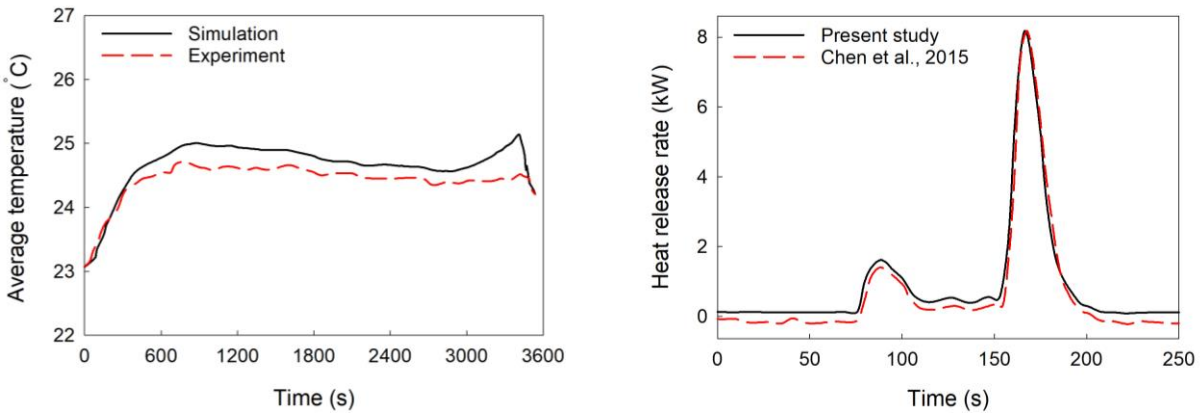


(a) Average temperature of a battery module (b) Heat release rate from a battery cell

**Figure 3** Validation results of (a) average temperature of a battery module, and (b) heat release rate from a battery cell.

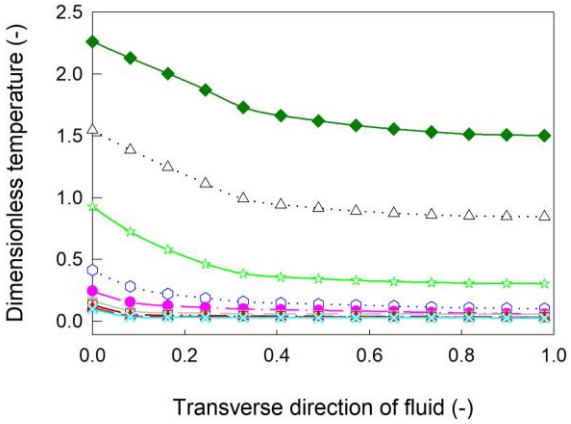


(a) Local temperature using an air coolant

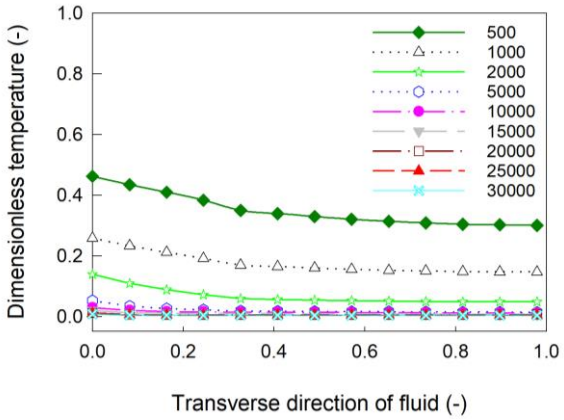


(b) Local temperature using a helium coolant

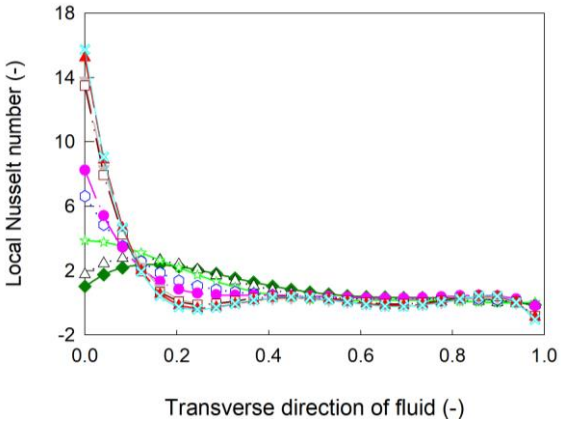


(c) Local Nusselt number using an air coolant

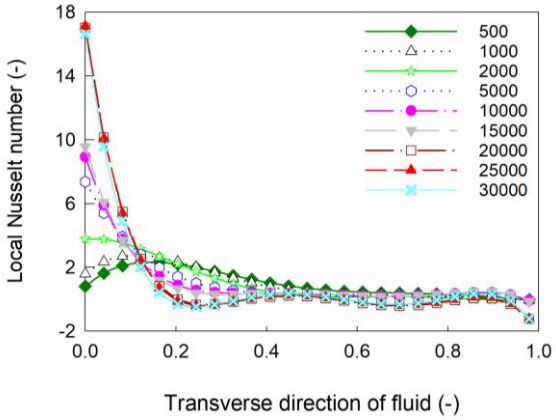


(d) Local Nusselt number using a helium coolant

**Figure 4** Distribution of local temperature and local Nusselt number along a flow channel with various Reynolds numbers using air and helium coolants.

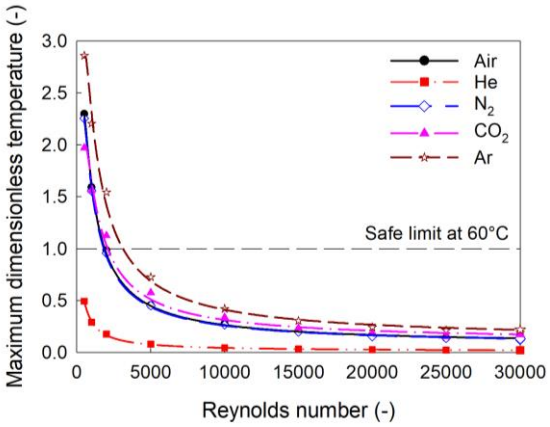


**Figure 5** Maximum dimensionless temperature at the battery surface with various Reynolds numbers and different gas coolants.

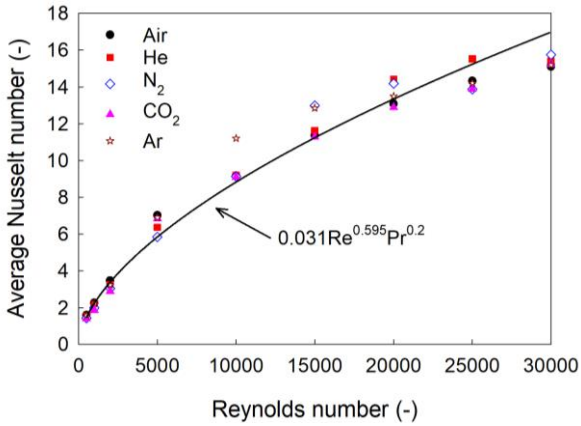


**Figure 6** Average Nusselt number with various Reynolds numbers using different coolants.

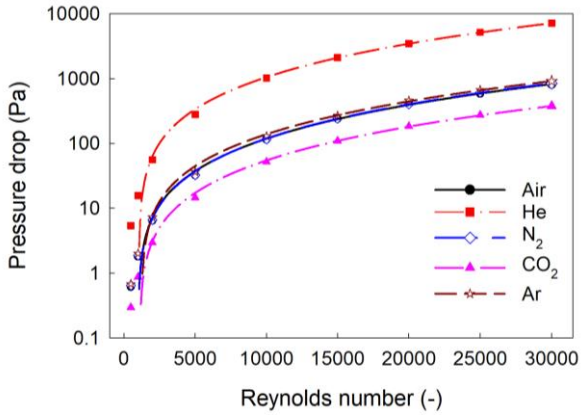


**Figure 7** Pressure drop of the system with different gas coolants.

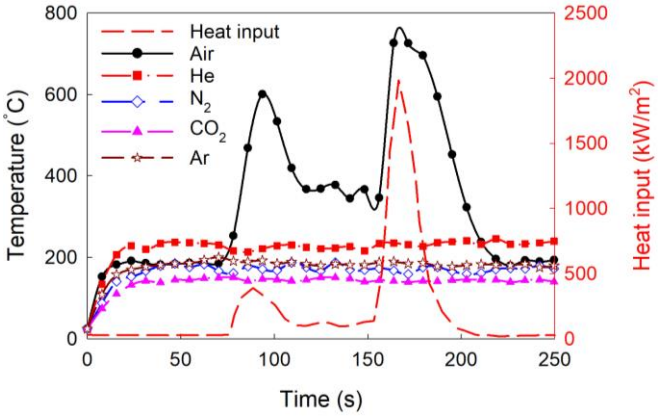


**Figure 8** Change in flame temperature with different gas coolants filled in an enclosure.

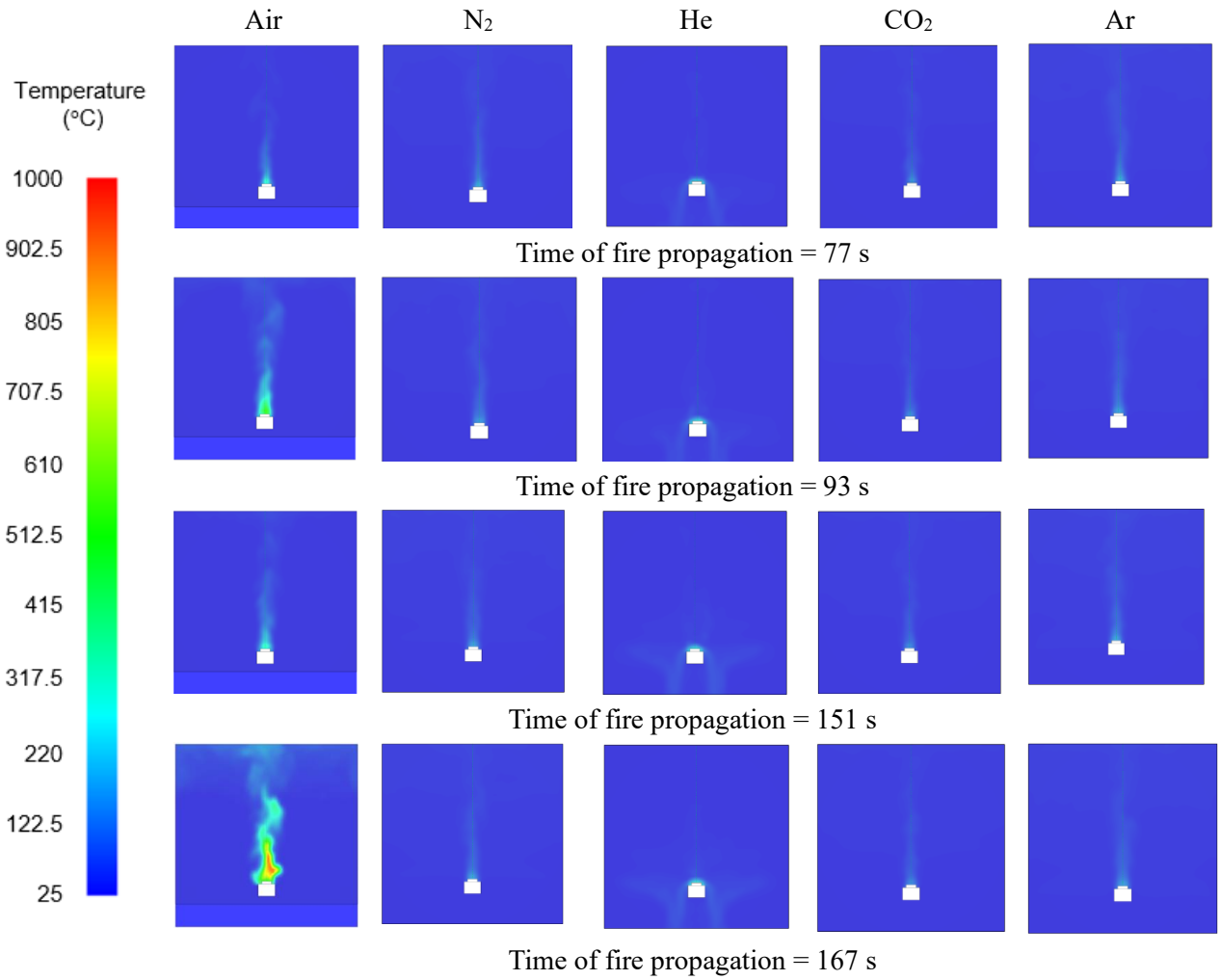


**Figure 9** Temperature distribution in a lithium-ion battery enclosure over time filled with five different gases.